

# Sensitivity considerations in polarization transfer and filtering using dipole–dipole couplings: Implications for biomineral systems

Sean C. Christiansen<sup>a</sup>, Niklas Hedin<sup>a</sup>, Jan D. Epping<sup>a</sup>, Michael T. Janicke<sup>a</sup>, Yolanda del Amo<sup>b</sup>, Mark Demarest<sup>b</sup>, Mark Brzezinski<sup>b</sup>, Bradley F. Chmelka<sup>a,\*</sup>

<sup>a</sup>Department of Chemical Engineering, University of California, Santa Barbara, CA 93106, USA

<sup>b</sup>Department of Ecology, Evolution, and Marine Biology, University of California, Santa Barbara, CA 93106, USA

Received 23 July 2005; received in revised form 19 October 2005

## Abstract

The robustness and sensitivities of different polarization-transfer methods that exploit heteronuclear dipole–dipole couplings are compared for a series of heterogeneous solid systems, including polycrystalline tetrakis(trimethylsilyl)silane (TKS), adamantane, a physical mixture of doubly <sup>13</sup>C,<sup>15</sup>N-enriched and singly <sup>13</sup>C-enriched polycrystalline glycine, and a powder sample of siliceous marine diatoms, *Thalassiosira pseudonana*. The methods were analyzed according to their respective frequency-matching spectra or resultant signal intensities. For a series of <sup>13</sup>C{<sup>1</sup>H} cross-polarization experiments, adiabatic passage Hartmann–Hahn cross-polarization (APHH-CP) was shown to have several advantages over other methods, including Hartmann–Hahn cross-polarization (HHCP), variable-amplitude cross-polarization (VACP), and ramped-amplitude cross-polarization (RACP). For X–Y systems, such as <sup>13</sup>C{<sup>15</sup>N}, high and comparable sensitivities were obtained by using APHH-CP with Lee–Goldburg decoupling or by using the transferred-echo double resonance (TEDOR) experiment. The findings were applied to multinuclear <sup>1</sup>H, <sup>13</sup>C, <sup>15</sup>N, and <sup>29</sup>Si CP MAS characterization of a powder diatom sample, a challenging inorganic–organic hybrid solid that places high demands on NMR signal sensitivity.

© 2005 Elsevier Inc. All rights reserved.

**Keywords:** Heteronuclear dipole–dipole couplings; Cross-polarization; Polarization transfer efficiency; Signal sensitivity; Glycine; Diatoms; <sup>13</sup>C CP MAS; <sup>15</sup>N CP MAS; <sup>29</sup>Si CP MAS; TEDOR

## 1. Introduction

It is widely appreciated that NMR signals of dilute nuclei or of nuclei with low gyromagnetic ratios or long  $T_1$  relaxation times can be enhanced by cross-polarization (CP) from abundant nuclear spins (typically protons) [1,2]. This enhancement is particularly useful if carried out under conditions of fast magic-angle spinning (MAS) to improve spectral resolution [3,4]. Although the predominant uses of cross-polarization techniques continue to involve nuclei with spin  $I = 1/2$ , increasing attention is also being directed toward half-integer quadrupolar nuclei [5–11]. In addition to desirable signal enhancement, CP can also be used for spectral editing [12–17] by selectively observing those nuclei that are dipole–dipole coupled (and therefore

in spatial proximity). Heteronuclear <sup>1</sup>H–X dipole–dipole spin couplings can be used to characterize local material structures, although the small <sup>1</sup>H chemical shift range (ca. 10 ppm) often leads to poorly resolved signals. In crystalline solids or materials with high extents of local ordering, resolution can be enhanced by the use of <sup>1</sup>H decoupling techniques [18–20]. However, in heterogeneous solids without such ordering or containing complicated compositions and/or distributions of organic species, insufficient <sup>1</sup>H NMR chemical shift resolution often makes it challenging to establish the identities of coupled spin species, even in two-dimensional experiments.

In instances where NMR-active non-proton spin species X and Y are also (or instead) present in a solid material, X–Y dipole–dipole couplings can be probed to take advantage of their typically larger chemical shift ranges (compared to <sup>1</sup>H) to obtain increased resolution for identifying coupled spin pairs. X–Y dipole–dipole

\*Corresponding author. Fax: +1 805 893 4731.

E-mail address: [bradc@engineering.ucsb.edu](mailto:bradc@engineering.ucsb.edu) (B.F. Chmelka).

interactions, however, are often weak due to the low gyromagnetic ratios and, in many cases, low natural abundances of the nuclei involved. These impediments can pose serious limitations towards the use of  $X$ – $Y$  dipole–dipole spin couplings and motivate efforts to increase resultant signal intensity. After the initial cascade-enhancement experiment [21], more advanced NMR techniques that rely on heteronuclear polarization transfer, including double cross-polarization (DCP) [22–25], transferred-echo double resonance (TEDOR) [26,27] and methods based on different dipolar recoupling techniques [28–33], have been introduced. The possibilities provided by such techniques for probing dipole–dipole couplings between distinct  $X$ – $Y$ , as well as  $^1\text{H}$ – $X$ , nuclei render these methods valuable for structural studies of heterogeneous solids.

Heteronuclear polarization-transfer techniques have previously been applied to a broad range of heterogeneous solids [34], including systems with commingled or interfacial inorganic–organic components. For example, TRAnSfer of Populations in DOuble Resonance (TRAPDOR) experiments [35] have provided information on the geometries of Al–H interactions associated with Brønsted acid sites in zeolites [36] and reverse cross-polarization to protons and Rotational-Echo DOuble Resonance (REDOR) experiments [37] have been used to examine hydrogen bonding of organic adsorbents to such sites [38,39]. Fyfe et al. have analyzed the three-dimensional structures formed between adsorbed organic molecules and zeolite frameworks [40,41] by cross-polarizing from protons in partially deuterated organic species, e.g., *p*-xylene, to  $^{29}\text{Si}$  framework sites. Cross-polarization from protons of organic template molecules to  $^{29}\text{Si}$  framework moieties has similarly been exploited to monitor the formation of the zeolite ZSM-5 in the presence of organic structure-directing agents [42]. In these studies, cross-polarization was predominantly achieved by applying spin-lock pulses with constant field strengths, often referred to as Hartmann–Hahn cross-polarization (HHCP). Two-dimensional (2D) HETeronuclear chemical shift CORrelation (HETCOR) measurements [43] have been used to investigate inorganic–organic interfaces in surfactant-templated mesoporous silicas and aluminosilicas [44–46], as well as in mesoporous silica particles [47].  $^{29}\text{Si}\{^{29}\text{Si}\}$  homonuclear dipole–dipole couplings have furthermore been exploited to examine intraframework structural ordering in zeolites [48] and surfactant-templated silicates [49], complementing earlier  $^{29}\text{Si}\{^{29}\text{Si}\}$  homonuclear scalar coupling measurements [46,50–52].

In contrast to the widespread use of heteronuclear polarization-transfer NMR methods for investigations of heterogeneous nano- and mesoporous inorganic solids, there are far fewer such studies in the literature on biogenic silicas or other biominerals [54–55]. Biogenic inorganic solids impose several serious challenges upon solid-state measurements of heteronuclear dipole–dipole couplings. First of all, their relatively dense structures result in lower

surface areas [56,57], compared to the heterogeneous nano- or mesoporous solids described above. This leads to a relatively low abundance of, for example, interfacial organic and inorganic species that might be cross-polarized. In addition, the nature and mixture of the biomolecule species/moieties involved in the organization and deposition of biosilica is expected to be diverse and exceedingly complex. Moreover, only a small fraction of such biomolecules or moieties may interact directly with the silica framework. The diversity of organic moieties present in samples of biological origin, together with the limited chemical shift range of protons, contributes furthermore to resolution challenges in experiments that rely on  $^1\text{H}$ – $X$  interactions. While it may be desirable for resolution reasons to consider polarization transfer techniques that exploit  $X$ – $Y$  dipole–dipole couplings, such as between  $^{29}\text{Si}$  and  $^{13}\text{C}$  or  $^{15}\text{N}$  nuclei, this approach places an even greater demand on the sensitivity of the NMR methodology selected. To confront these issues, it is important and desirable to apply solid-state heteronuclear polarization-transfer methods that yield both high sensitivity and high resolution. Here, the relative sensitivities of different resolution-enhancement techniques that exploit heteronuclear dipole–dipole couplings are examined on several model compounds to compare their relative efficacies for detecting and filtering signals among coupled spin pairs. The insights are subsequently applied to the characterization of biogenic silica from a species of diatoms, a challenging heterogeneous solid system.

## 2. Materials and methods

### 2.1. Samples

Sensitivity and robustness of  $^{13}\text{C}\{^1\text{H}\}$  cross-polarization techniques were investigated on solid tetrakis(trimethylsilyl)silane (TKS:  $[(\text{CH}_3)_3\text{Si}]_4\text{Si}$ , 98%, Aldrich) and adamantane ( $\text{C}_{10}\text{H}_{16}$ , Aldrich).

Selective filtering through the use of heteronuclear dipole–dipole couplings was investigated by using a sample obtained by physically mixing powders of two isotopically labeled compounds of polycrystalline glycine, one singly enriched in  $^{13}\text{C}$  at the carboxylic site ( $1\text{-}^{13}\text{C}$  glycine:  $\text{H}_2\text{N}-\text{CH}_2\text{-}^{13}\text{COOH}$ , 99%  $^{13}\text{C}$ ) and the other doubly enriched both in  $^{13}\text{C}$  at the methylene site and in  $^{15}\text{N}$  at the amine moiety ( $2\text{-}^{13}\text{C}$ ,  $^{15}\text{N}$  glycine:  $\text{H}_2^{15}\text{N}-^{13}\text{CH}_2\text{-COOH}$ , 99%  $^{13}\text{C}$ , 98% +  $^{15}\text{N}$ ). The isotopically labeled glycine compounds were used as-received from Cambridge Isotope Laboratories (Andover, Massachusetts, USA). The physical mixture was prepared by combining 40 wt% of the singly labeled glycine with 60 wt% of the doubly labeled compound.

A unialgal and axenic culture of *Thalassiosira pseudonana* (clone 3H-CCMP 1335) was obtained from the Provasoli-Guillard National Center for Culture of Marine

Phytoplankton (CCMP) at the Bigelow Marine Laboratory for Ocean Sciences (Maine, USA). It was maintained in  $f/2$  enriched seawater medium with added dissolved silicon at 17 °C under a continuous light of approximately  $100 \text{ mEm}^{-2} \text{ s}^{-1}$  as previously described in [58,59]. 200 ml of the culture were initially grown in nutrient enriched  $f/2$  seawater media with Si:N and N:P ratios of 1:18 and 24:1, respectively, to avoid nitrogen and phosphorous limitation during growth [60]. When cell densities reached 500,000 cells/ml, the diatom inoculum was transferred to an automated mass culturing system, which allows for cell densities 24–45 times greater than conventional methods ( $10^8$  cells/ml in 10 days). Isotopically enriched  $\text{SiO}_2$  ( $^{29}\text{Si}$ , 96%+, Oak Ridge National Laboratory, Tennessee, USA),  $\text{NaHCO}_3$  ( $^{13}\text{C}$ , 99%, Cambridge Isotope Laboratories) and  $\text{NaNO}_3$  ( $^{15}\text{N}$ , 98%+, Cambridge Isotope Laboratories) were supplied to the cell culture to produce diatoms that were isotopically enriched in  $^{29}\text{Si}$ ,  $^{13}\text{C}$ , and/or  $^{15}\text{N}$ . To remove excess organic species unassociated with the silica network, some diatom samples were subjected to sonication and subsequent centrifugation. The samples were then centrifuged to pellets and lyophilized (dried), as well as dehydrated at room temperature under  $1.3 \times 10^{-3}$  Pa to remove additional water present.

## 2.2. NMR measurements

$^{13}\text{C}\{^1\text{H}\}$  CP MAS spectra of TKS were recorded on a Chemagnetics CMX-180 spectrometer using a widebore 4.2 T superconducting magnet under conditions of MAS with spinning speeds of 6 kHz. All other NMR spectra were recorded on a Chemagnetics CMX-500 spectrometer using a widebore 11.7 T superconducting magnet and a triple-resonance magic-angle-spinning probehead with 5.0 mm Pencil<sup>TM</sup> rotors.  $^{13}\text{C}\{^{15}\text{N}, ^1\text{H}\}$  CP MAS experiments (9 kHz) were performed on the physically mixed sample of two differently labeled compounds of polycrystalline glycine: 40 wt% 1- $^{13}\text{C}$  glycine ( $\text{H}_2\text{N}-\text{CH}_2-^{13}\text{COOH}$ , 99%  $^{13}\text{C}$ ) and 60 wt% 2- $^{13}\text{C}$ ,  $^{15}\text{N}$  glycine ( $\text{H}_2^{15}\text{N}-^{13}\text{CH}_2-\text{COOH}$ , 99%  $^{13}\text{C}$ , 98%+  $^{15}\text{N}$ ) using a 5 s pulse delay with 64 transients recorded for each spectrum. Cross-polarization experiments were optimized for Hartmann–Hahn matching conditions  $\gamma_I B_I = \gamma_S B_S$  or the Hartmann–Hahn mismatch condition  $\gamma_I B_I = \gamma_S B_S + n\omega_R$ .  $^{13}\text{C}\{^1\text{H}\}$  and  $^{13}\text{C}\{^{29}\text{Si}, ^1\text{H}\}$  CP MAS spectra of a doubly enriched [ $^{13}\text{C}$ (85%),  $^{29}\text{Si}$ (98%)] or triply enriched [ $^{13}\text{C}$ (85%),  $^{29}\text{Si}$ (98%),  $^{15}\text{N}$ (98%)] diatom species *T. pseudonana* were recorded at room temperature and  $-50$  °C, respectively, under MAS conditions at 4 kHz. The  $^{15}\text{N}\{^1\text{H}\}$  CP MAS spectrum was recorded at room temperature under conditions of MAS at 5 kHz with 20,400 signal-averaged transients. The  $^{29}\text{Si}\{^1\text{H}\}$  HETCOR spectrum was acquired at room temperature applying a 2 ms contact pulse under MAS at 5 kHz.  $^1\text{H}$ ,  $^{13}\text{C}$  and  $^{29}\text{Si}$  NMR chemical shifts are referenced to tetramethylsilane,  $(\text{CH}_3)_4\text{Si}$ , and the  $^{15}\text{N}$  NMR chemical shifts to nitromethane,  $\text{CH}_3\text{NO}_2$ .

## 3. Results and discussion

Investigations of inorganic–organic interfaces in biomineral samples are challenging, due to their low surface areas and the complicated mixtures of organic moieties present, only a small fraction of which furthermore interact directly with the inorganic framework. Such systems are expected to be beneficially examined by solid-state NMR, for example, through the use of heteronuclear polarization-transfer MAS methods, to enhance the sensitivity and resolution of signals that are associated particularly with interfacial species of interest. The inherently low abundances and complex compositions of inorganic–organic species at biomineral surfaces, however, place extraordinary demands on signal sensitivity and resolution that both must be maximized to detect dilute interfacial molecular moieties. To do so requires that the conditions needed to enhance spectral resolution, e.g., by magic-angle-sample spinning and combined application of selective polarization-transfer filters, be balanced against the need to maximize resulting signal sensitivity. High heteronuclear polarization-transfer efficiency is crucial for examining heterogeneous biomineral interfaces, as will be discussed in detail below. To achieve both high signal sensitivity and efficient polarization transfer selectivity, the conditions under which heteronuclear polarization transfer occurs must therefore be optimized.

### 3.1. Polarization transfer via $X-^1\text{H}$ heteronuclear dipolar couplings

A number of different heteronuclear cross-polarization methods are available, with different efficacies that markedly influence resultant signal intensity and separation. Notably, measurements performed under conditions of MAS yield increased spectral resolution, but impose extra complexity on the responses of the associated nuclei to radio frequency excitation. The cross-polarization process depends on heteronuclear dipole–dipole interactions, which can be considered to be effectively static provided the  $^1\text{H}-^1\text{H}$  dipolar fluctuations are much larger than the oscillations introduced by sample rotation [61]. While this is the case for sufficiently slow spinning speeds, it is well known that faster rates of rotation impose oscillatory behavior(s) on the heteronuclear dipolar interactions that govern such cross-polarization processes [62]. Fig. 1, for example, illustrates the influence of the MAS spinning frequency on the  $^{13}\text{C}$  CP matching spectrum of TKS, showing large variations in signal intensities. Under static sample conditions,  $^1\text{H}$  homonuclear dipole–dipole couplings result in a  $^1\text{H}$  NMR linewidth (FWHM) of approximately 5300 Hz. Under MAS conditions, the FWHM linewidth decreases to 850 Hz, indicating that the sample rotation frequency is of the order of the  $^1\text{H}$  homonuclear dipolar couplings. The  $^{13}\text{C}$  CP matching spectra in Figs. 1(b–d) reveal highly non-uniform intensity profiles with frequency bands that point to the benefit of

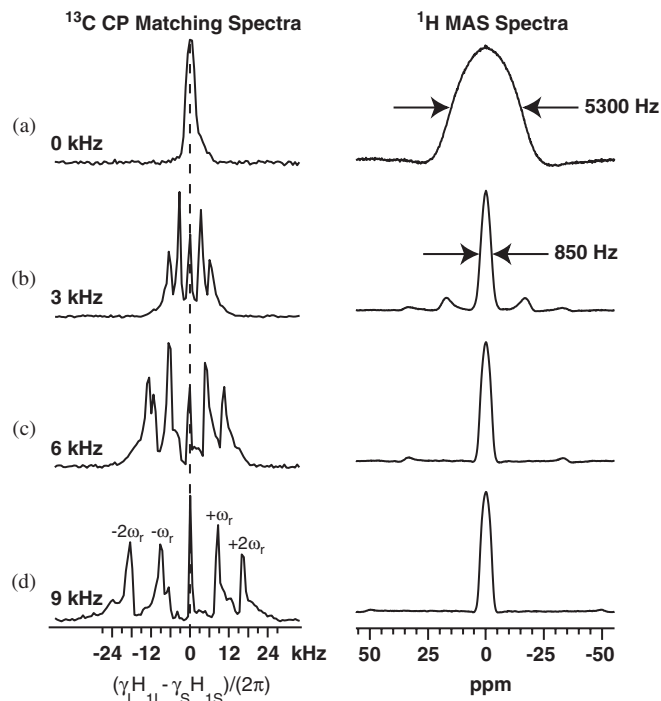


Fig. 1.  $^{13}\text{C}$  CP matching spectra and the corresponding solid-state  $^1\text{H}$  NMR spectra of tetrakis(trimethylsilyl)silane (TKS) at 4.2 T under (a) static and MAS conditions at: (b) 3 kHz, (c) 6 kHz, and (d) 9 kHz.

using modified Hartmann–Hahn conditions. Under fast MAS conditions, intensity bands in the CP matching spectra at integer multiples of the sample rotation frequency  $\pm n\omega_r$  arise from cross-polarization via through-space dipole–dipole-coupled  $^1\text{H}$  nuclei; the intensity at frequency band  $n = 0$  arises from cross-polarization from covalently attached protons via through-bond  $J$ -couplings [63]. Cross-polarization experiments can, thus, be used to differentiate between through-bond and through-space interactions to distinguish between covalently bonded and other spatially proximate moieties.

Nevertheless, the relatively narrow maxima and deep minima of CP matching spectra create difficult conditions for polarization transfer under MAS, which is often vital for obtaining sufficient resolution in solids, including inorganic–organic biomineral composites. Different cross-polarization methods overcome these challenges to differing extents, which are important to evaluate, especially when signal sensitivity is of high concern. A number of pulse sequences, for example, have been proposed to broaden the narrow, discrete matching conditions by modulating the spin-lock field profile [64]. Fig. 2 shows a comparison of the spin-lock field profiles of different cross-polarization techniques and their corresponding  $^{13}\text{C}$  CP matching spectra under conditions of MAS at 6 kHz. The standard HHCP sequence, using a constant spin-lock field strength, is shown along with its resulting spectrum in Fig. 2(a). The constant spin-lock field strength makes HHCP straightforward to implement, but yields an overall lower CP efficiency compared to other methods, due to its

narrow matching conditions. By comparison, the more advanced variable-amplitude cross-polarization (VACP) sequence [65,66], shown in Fig. 2(b), is composed of a number of shorter spin-lock fields with incrementally decreasing or increasing amplitudes. The use of various spin-lock fields in one experiment yields a broad maximum in the  $^{13}\text{C}$  CP matching spectrum, with weak fluctuations due to the fast sample spinning. However, the rapid changes in field-amplitude place high demands on the amplifiers. The ramped-amplitude cross-polarization (RACP) method [67] (Fig. 2(c)) also produces a broad matching spectrum, but uses a monotonically increasing field-lock profile, which is less demanding on amplifier equipment. The RACP sequence yields best cross-polarization efficiencies when the center of the ramped spin-lock field is located at one of the relative intensity maxima of the CP matching spectrum.

The most-efficient CP MAS experiments to date use adiabatic passage Hartmann–Hahn cross-polarization (APHH-CP) techniques [68,69], which rely on a tangential spin-lock field profile that depends on the strength of the heteronuclear and homonuclear dipole–dipole couplings and the spinning speed. In contrast to the sequences discussed previously, the APHH-CP sequence is performed at only one of the intensity maxima observed in a conventional HHCP matching spectrum (e.g., Fig. 2(a)). As a consequence, a CP matching spectrum for various spin-lock positions is not meaningful for this sequence. Although the APHH-CP experiment requires extensive preparatory efforts to setup, the signal intensity obtained by APHH-CP techniques is near the theoretical maximum that can be achieved by CP experiments [69,70]. Fig. 3 shows that the adamantane  $^{13}\text{C}\{^1\text{H}\}$  spectrum acquired using the APHH-CP sequence with a sweep over the  $+\omega_r$  frequency maximum has nearly twice the intensity (Fig. 3(b)), as compared to the HHCP spectrum under the same conditions (Fig. 3(a)). Under the fast MAS conditions required for  $^{29}\text{Si}\{^1\text{H}\}$  CP studies of biosiliceous diatoms (see below), the APHH-CP technique similarly yields the highest sensitivity among the methods examined.

### 3.2. Polarization transfer via $X$ – $Y$ heteronuclear dipolar couplings

For many complicated and heterogeneous solids, including inorganic–organic biomineral composites, it is advantageous to exploit heteronuclear  $X$ – $Y$  (non- $^1\text{H}$ ) dipolar interactions to increase spectral resolution and/or selectivity. One particularly powerful approach is to incorporate an  $X$ – $Y$  heteronuclear dipolar filter to cross-polarize and then select nuclei involved in such coupled spin pairs. Sensitivity, again, is often of paramount importance, because one or both of the nuclei may be rare-spins with low abundances or low gyromagnetic ratios. To compare the performances of NMR pulse sequences that probe  $X$ – $Y$  heteronuclear dipole–dipole couplings,  $^{13}\text{C}$  NMR spectra were acquired on a physical powder mixture (40:60 mass

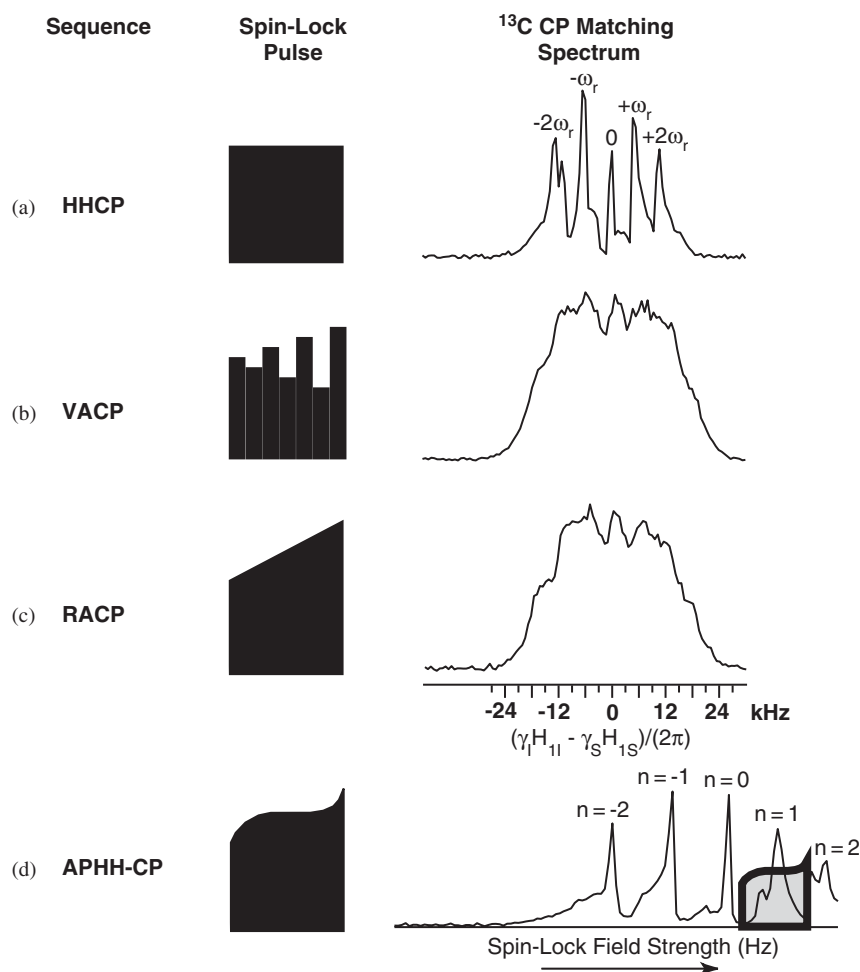


Fig. 2.  $^{13}\text{C}$  CP matching spectra performed with different spin-lock field profiles on TKS under MAS at 6 kHz. (a) The Hartmann–Hahn cross-polarization (HHCP) spectrum, showing significant intensity variations. By comparison, the (b) variable amplitude cross-polarization (VACP) and (c) ramped-amplitude cross-polarization (RACP) sequences yield broader matching spectra and substantially reduce the intensity variations. (d) The adiabatic passage Hartmann–Hahn cross-polarization (APHH-CP) sequence provides good signal sensitivity, though is designed to be performed only at the frequency  $+\omega_r$  and so cannot strictly be compared for other spin-lock field strengths.

ratio) of two different isotopically labeled, but otherwise identical, compounds of polycrystalline glycine: 1- $^{13}\text{C}$  glycine ( $\text{H}_2\text{N}-\text{CH}_2-^{13}\text{COOH}$ , 99%  $^{13}\text{C}$ ) singly  $^{13}\text{C}$  enriched at the carboxylic site and 2- $^{13}\text{C}$ ,  $^{15}\text{N}$  glycine ( $\text{H}_2^{15}\text{N}-^{13}\text{CH}_2-\text{COOH}$ , 99%  $^{13}\text{C}$ , 98%+  $^{15}\text{N}$ ) doubly enriched in  $^{13}\text{C}$  at the methylene site and in  $^{15}\text{N}$  at the amine site. The  $^{13}\text{C}\{^1\text{H}\}$  CP MAS spectrum acquired on this sample, using a standard HHCP sequence with continuous wave decoupling, is shown in Fig. 4(a). The spectrum displays two resonances arising from the two distinct  $^{13}\text{C}$ -enriched moieties, with their relative intensities (including spinning sidebands) corresponding to their respective populations in the physical powder mixture. The resonance at 175 ppm arises from the carboxylic species of the singly  $^{13}\text{C}$ -enriched glycine molecules, and the resonance at 42 ppm arises from the methylene carbon moiety of the doubly enriched  $^{13}\text{C}$ ,  $^{15}\text{N}$  glycine molecules.

Using pulse sequences based on cross-polarization from  $^{15}\text{N}$  to  $^{13}\text{C}$ , however, only  $^{13}\text{C}$  nuclei that are dipole–dipole

coupled to  $^{15}\text{N}$  nuclei are observed, leading to only one  $^{13}\text{C}$  resonance at 42 ppm.  $^{13}\text{C}\{^{15}\text{N}\}$  cross-polarization experiments were performed on the 40:60 physical powder mixture of singly  $^{13}\text{C}$ -enriched and doubly  $^{13}\text{C}$ ,  $^{15}\text{N}$ -enriched polycrystalline glycine using a series of different methods to compare their relative sensitivities. Except for the use of the different pulse sequences, all other experimental conditions were the same. All of the experiments used initial cross-polarization from  $^1\text{H}$  to  $^{15}\text{N}$  nuclei via a standard HHCP sequence to increase the polarization of the  $^{15}\text{N}$  nuclei,<sup>1</sup> followed by transfer of  $^{15}\text{N}$  magnetization to dipole–dipole-coupled  $^{13}\text{C}$  nuclei, according to the different pulse-schemes.

The simplest and most widely used method for heteronuclear  $X$ – $Y$  cross-polarization, such as between  $^{13}\text{C}$  and  $^{15}\text{N}$  spin pairs, is commonly referred to as double cross-polarization (DCP) [22–24]. In this

<sup>1</sup>Additional signal intensity could be gained in each case by using adiabatic cross-polarization from  $^1\text{H}$  to  $^{15}\text{N}$ .

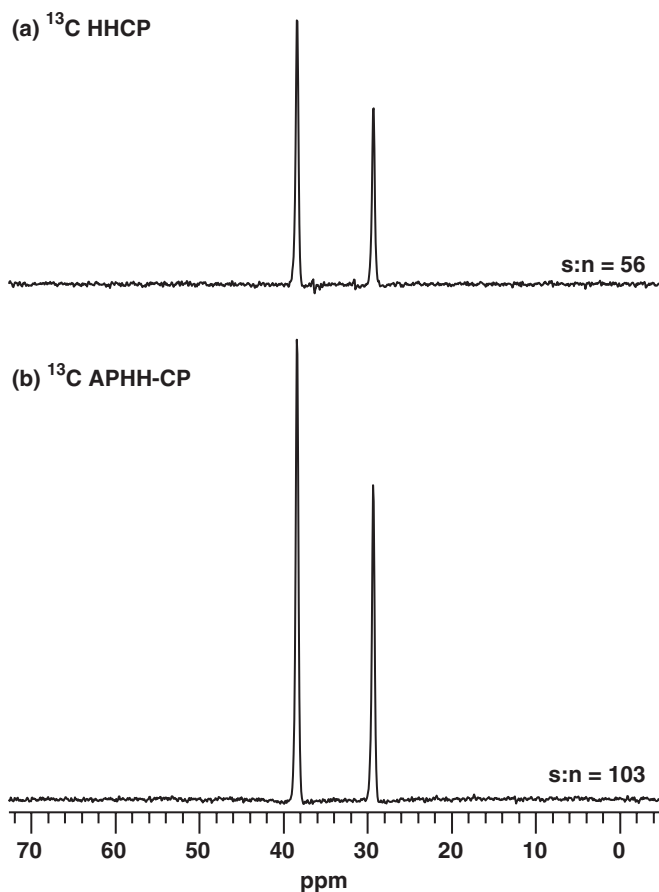


Fig. 3.  $^{13}\text{C}$  CP MAS spectra of adamantane performed under MAS conditions at 6 kHz using (a) a standard constant amplitude spin-lock CP sequence (HHCP) and (b) an adiabatic passage Hartmann–Hahn cross-polarization sequence (APHH-CP).

experiment (shown schematically in Fig. 4(b)), initially prepared proton magnetization is transferred to dipole–dipole-coupled  $^{15}\text{N}$  nuclei, after which the  $^{15}\text{N}$  magnetization is again transferred to dipole–dipole-coupled  $^{13}\text{C}$  nuclei. The  $^{15}\text{N}$ – $^{13}\text{C}$  transfer is achieved by using a rectangular-shaped constant-field-strength spin-lock profile, and the  $^{13}\text{C}$  NMR spectrum is subsequently acquired while applying continuous-wave decoupling via the proton channel.  $^1\text{H}$  decoupling is not applied during the  $^{15}\text{N}$ – $^{13}\text{C}$  contact pulse and thus  $^1\text{H}$ – $^{13}\text{C}$  magnetization transfer may also occur, although under conditions of MAS and the  $^{13}\text{C}$  contact pulse,  $^1\text{H}$ – $^{13}\text{C}$  interactions will be diminished. The DCP sequence is widely used, due to its straightforward implementation and relative insensitivity to distributions of powder crystallite angles (referred to as ‘ $\gamma$ -encoding’ [71]). As shown in Fig. 4(b) for the 40:60 polycrystalline physical mixture of singly ( $^{13}\text{C}$ ) and doubly ( $^{13}\text{C}$ ,  $^{15}\text{N}$ ) labeled glycine powders, the DCP pulse sequence results in a  $^{13}\text{C}$  spectrum with *no* measurable signal intensity.<sup>2</sup> It is clear that, in this particular sample, the

$^{15}\text{N}$ – $^{13}\text{C}$  dipolar couplings are sufficiently weak that a more sensitive means for exploiting and detecting heteronuclear couplings is required.

One way to improve the signal intensity achieved from a heteronuclear dipole–dipole-selective experiment is to use techniques that rely on modulated, rather than constant (DCP), spin-lock field strengths for polarization transfer between  $X$  and  $Y$  nuclei. Based on the significant intensity enhancement obtained for cross-polarization from protons to  $X$  nuclei provided by APHH-CP (Fig. 3), this approach was selected for analogous transfer of polarization between  $X$ – $Y$  nuclei [75]. As shown in Fig. 4(c), this can be achieved by transferring the initially prepared proton magnetization to  $^{15}\text{N}$  nuclei (as before), followed by the application of a tangential spin-lock profile to the  $^{13}\text{C}$  channel to initiate APHH-CP transfer of magnetization between coupled  $^{15}\text{N}$  and  $^{13}\text{C}$  nuclei. The variable intensity of the adiabatic spin-lock pulse also provides sequential matching across different CP conditions, effectively eliminating undesirable effects from magnetic field inhomogeneities and chemical shift offsets, thereby augmenting signal intensity still further. An additional, general challenge associated with  $X$ – $Y$  cross-polarization in organic, polymeric, or biological samples is the often complicating influence of the strongly-coupled proton spin system. Besides the resolution difficulties that corresponding  $^1\text{H}$ – $X$  and/or  $^1\text{H}$ – $Y$  dipole–dipole couplings present, residual  $^1\text{H}$ – $^1\text{H}$  interactions can also induce undesirable relaxation effects in  $X$ – $Y$  spin systems during the spin-lock contact period, and thereby decrease cross-polarization efficiency [70,75]. To reduce these effects, continuous-wave  $^1\text{H}$  decoupling can be applied during the  $^{15}\text{N}$ – $^{13}\text{C}$  contact pulse, as well as during the acquisition period, as shown in Fig. 4(c). Under these conditions, for the polycrystalline glycine mixture at hand, the APHH-CP method yields a strong  $^{13}\text{C}$  signal at 42 ppm from the methylene carbon atoms of the doubly  $^{13}\text{C}$ ,  $^{15}\text{N}$ -enriched glycine species with a signal-to-noise ratio of 32.5. This is in contrast to the DCP  $^{13}\text{C}$  spectrum without  $^1\text{H}$  decoupling during the  $^{15}\text{N}$ – $^{13}\text{C}$  contact pulse (Fig. 4(b)) for which no signal was detected. It is important also to note that no signal is observed at 175 ppm, showing that the heteronuclear  $^{15}\text{N}$ – $^{13}\text{C}$  filter effectively excludes signals from the  $^{13}\text{C}$ -enriched carboxylic groups of the singly labeled glycine.

The effects from residual  $^1\text{H}$ – $^1\text{H}$  interactions may be particularly important in the APHH-CP experiment, due to the longer contact times required for the adiabatic sweep, compared to other cross-polarization methods [68]. This disadvantage of the APHH-CP method can nevertheless be overcome by incorporating Lee–Goldburg (LG) decoupling [76], instead of continuous-wave (CW) decoupling, during the  $^{15}\text{N}$ – $^{13}\text{C}$  contact pulse [75].

(footnote continued)

CP (SPICP) [72], RF-driven recoupling in CP (RFDRCP) [73] and improved double CP (iDCP) [74]. Such considerations are not expected to dominate the sensitivity and resolution limitations here.

<sup>2</sup>The DCP method also depends sensitively on anisotropic chemical shielding and resonance offset effects, which several recent experiments have been developed to overcome, including simultaneous phase-inversion

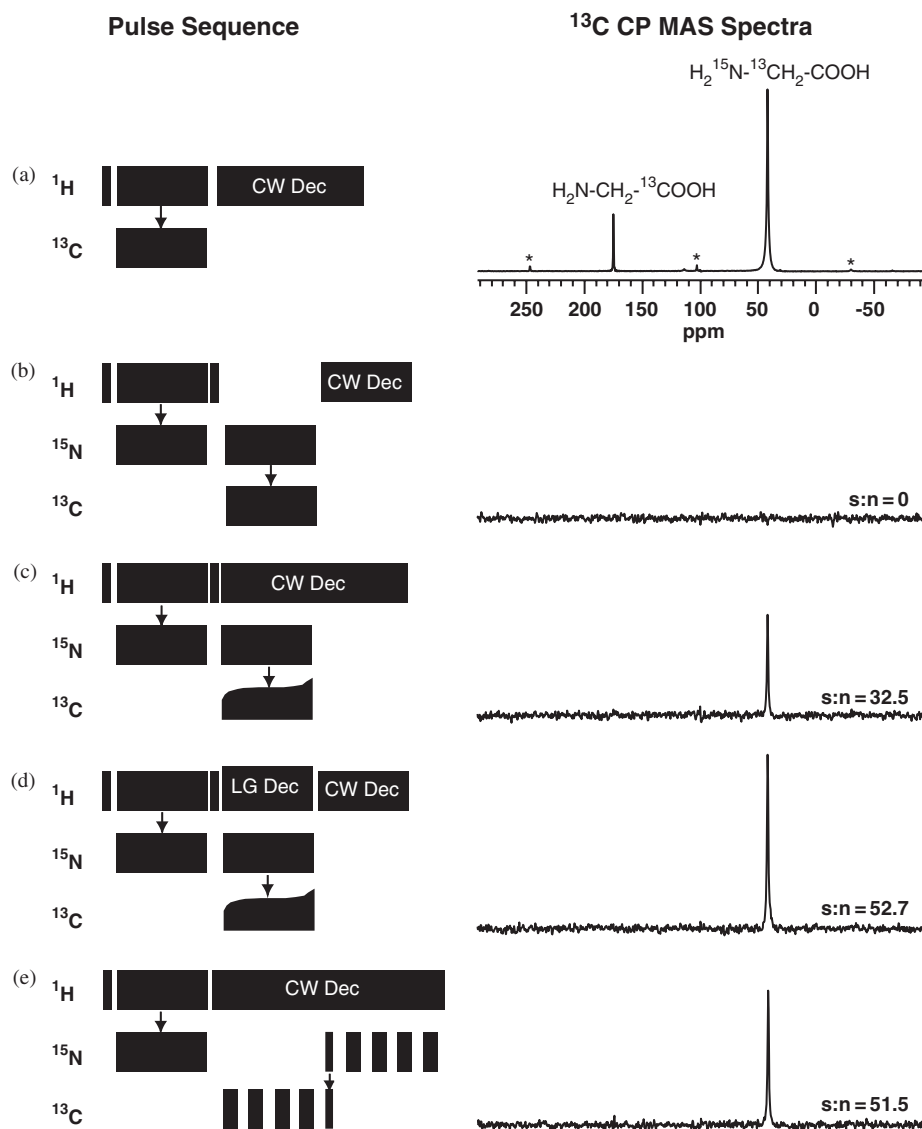


Fig. 4. Comparison of  $^{13}\text{C}$  MAS spectra obtained by using different heteronuclear  $^{13}\text{C}$ – $^{15}\text{N}$  polarization transfer pulse sequences on a physical mixture of 40 wt%  $1\text{-}^{13}\text{C}$  glycine ( $\text{H}_2\text{N-CH}_2\text{-}^{13}\text{COOH}$ , 99%  $^{13}\text{C}$ ) and 60 wt%  $2\text{-}^{13}\text{C}$ ,  $^{15}\text{N}$  glycine ( $\text{H}_2^{15}\text{N-}^{13}\text{CH}_2\text{-COOH}$ , 99%  $^{13}\text{C}$ , 98%  $^{15}\text{N}$ ). 5 (a) Standard HHCP cross-polarization sequence and (b–e) four different pulse sequences used to measure  $^{13}\text{C}$ – $^{15}\text{N}$  dipole–dipole couplings under MAS conditions at 9 kHz. Sequence (b) is the double cross-polarization (DCP) sequence, while (c) is the APHH-CP from  $^{15}\text{N}$  to  $^{13}\text{C}$ , with CW decoupling on the proton channel. Sequence (d) applies the same spin-lock field profile between  $^{15}\text{N}$  and  $^{13}\text{C}$ , but with Lee–Goldburg decoupling on the proton channel during the  $^{15}\text{N}$ – $^{13}\text{C}$  contact time, while (e) is the transferred-echo double resonance (TEDOR) sequence. The integrated signal-to-noise ratio (s:n) is shown along with each spectrum.

Homonuclear Lee–Goldburg  $^1\text{H}$  decoupling uses a series of off-resonance  $^1\text{H}$  pulses to generate an effective ( $B_{1,\text{H}}$ ) field that is oriented at the magic-angle relative to the static ( $B_0$ ) field [76]. Compared to CW approaches, Lee–Goldburg decoupling reduces more effectively the influences of prevalent proton spin-couplings both to other protons and to other nearby  $^{13}\text{C}$  and  $^{15}\text{N}$  nuclei. This leads to improved efficiencies for  $^{15}\text{N}$ – $^{13}\text{C}$  polarization transfer and correspondingly increased signal intensities. Fig. 4(d) shows a pulse sequence that is identical to the APHH-CP sequence in Fig. 4(c), except for the inclusion of Lee–Goldburg decoupling in place of CW decoupling. For the mixed polycrystalline glycine sample, the Lee–

Goldburg APHH-CP experiment produces significantly enhanced  $^{13}\text{C}$  signal intensity, yielding a signal-to-noise ratio of 52.7. This represents a sensitivity increase of approximately 60%, compared to the APHH-CP measurement without Lee–Goldburg decoupling applied to the proton channel during the heteronuclear  $^{15}\text{N}$ – $^{13}\text{C}$  contact pulse.

A different approach to heteronuclear polarization transfer is achieved by the Transferred-Echo Double-Resonance (TEDOR) experiment, where recoupled dipole–dipole interactions are exploited under conditions of rapid MAS [24,27]. As shown in Fig. 4(e), following initial cross-polarization from  $^1\text{H}$  to  $^{15}\text{N}$  nuclei,

the TEDOR experiment uses a series of rotor-synchronized  $\pi$  pulses on the  $^{13}\text{C}$  channel to reintroduce dipole–dipole couplings between nearby  $^{13}\text{C}$  and  $^{15}\text{N}$  nuclei. This leads to a buildup of coherence on the  $^{15}\text{N}$  nuclei that can subsequently be transferred to  $^{13}\text{C}$  nuclei, through the application of  $\pi/2$  pulses simultaneously to both channels. The  $^{13}\text{C}$  polarization is then converted into observable magnetization by a series of rotor-synchronized  $\pi$  pulses on the  $^{15}\text{N}$  channel. For the glycine mixture at hand, the sensitivity of the TEDOR experiment (Fig. 4(e)) is comparable to that achieved by the APHH-CP experiment with Lee–Goldburg decoupling, yielding a  $^{13}\text{C}$  signal-to-noise ratio of 51.5.

The comparison of the different methods for achieving  $^{15}\text{N}$ – $^{13}\text{C}$  heteronuclear polarization transfer in a physical mixture of polycrystalline glycine powders shows that the APHH-CP with Lee–Goldburg decoupling and TEDOR experiments yield comparable signal sensitivities and are significantly more sensitive than the widely used DCP experiment. Of the two, the TEDOR experiment has the limitation of being most suitable for isolated ‘immobile’ spin pairs, which may limit its feasibility for complex heterogeneous systems with target nuclei in high abundances, where these conditions may not be valid. The APHH-CP pulse sequence with Lee–Goldburg decoupling appears to be generally applicable for efficient promotion of heteronuclear polarization transfer and detection of dipole–dipole-coupled systems.

### 3.3. $^{29}\text{Si}\{^1\text{H}\}$ , $^{13}\text{C}\{^{29}\text{Si}\}$ , and $^{15}\text{N}\{^{29}\text{Si}\}$ cross-polarization in labeled marine diatoms

Biomineral systems are particularly challenging heterogeneous solids that are comprised of regions of inorganic and organic components, whose interfacial interactions and compositions are largely unknown. Marine diatoms, single-cell photosynthetic algae, are examples of such systems, in which amorphous silica frustules are deposited and formed, apparently under genetic control, into elaborate hierarchically ordered structures with dimensions of several to hundreds of microns. Scanning electron microscopy (SEM) images for the diatom species *T. pseudonana* (see Section 2), for example, are shown in Fig. 5. Little is known about the compositions or structures of molecular components at the surface(s) of the silica frustules, largely due to the challenges of characterizing dilute interfacial organic species in biogenically derived silica. In these systems, low interfacial areas between organic and silica components demand maximum signal sensitivity, which can be augmented by high degrees of isotopic enrichment.

Fig. 6(a), for example, shows solid-state single-pulse (solid line) and  $^{29}\text{Si}\{^1\text{H}\}$  CP (dotted line) MAS NMR spectra of a doubly labeled  $^{29}\text{Si}$ ,  $^{13}\text{C}$ -enriched powder sample of the diatom species *T. pseudonana*. The spectra reveal three broad  $^{29}\text{Si}$  resonances centered at  $-94$ ,  $-102$ , and  $-112$  ppm attributed to  $Q^2$ ,  $Q^3$  and  $Q^4$   $^{29}\text{Si}$  species,

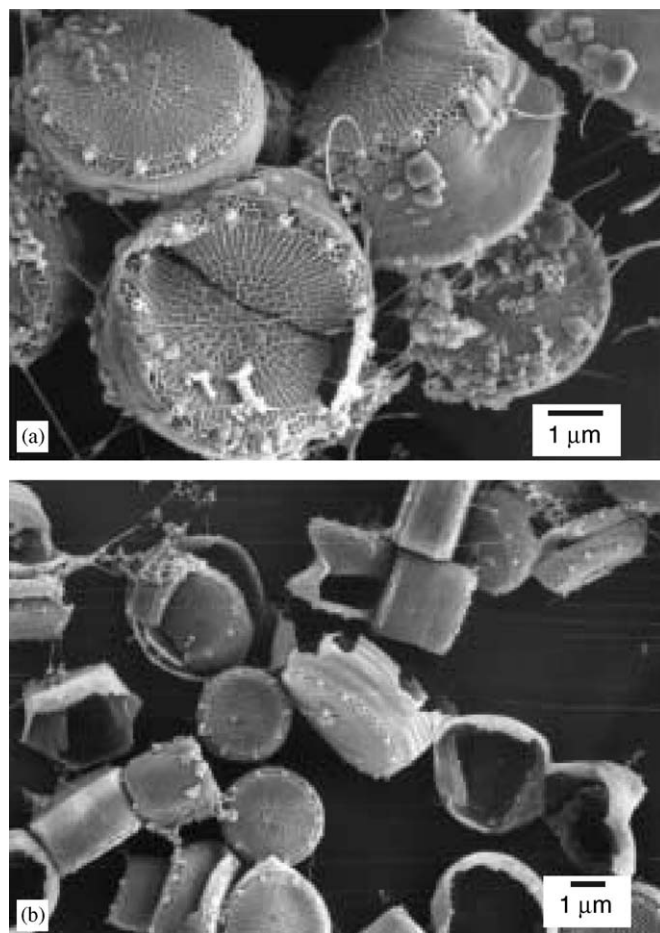


Fig. 5. Scanning electron microscope images of the diatom *Thalassiosira pseudonana* (a) prior to sonication and (b) after sonication.

respectively, corresponding to tetrahedrally coordinated  $Q^n$   $^{29}\text{Si}$  sites, with  $n$  nearest Si neighbors bonded covalently via bridging oxygen atoms [77]. The quantitative single-pulse  $^{29}\text{Si}$  MAS spectrum shows that the majority ( $\sim 76\%$ ) of silicon species present in the diatom frustule are fully cross-linked  $Q^4$  moieties, with a predominant remaining fraction ( $\sim 22\%$ ) of  $Q^3$  and a small amount ( $\sim 2\%$ ) of  $Q^2$  species, which is similar to  $^{29}\text{Si}$  VACP and single-pulse MAS results that have been recorded for other diatom species [78,79]. The  $^{29}\text{Si}\{^1\text{H}\}$  CP MAS spectrum confirms the presence of  $Q^3$  and  $Q^2$   $^{29}\text{Si}$  species by enhancing the signals from these species by magnetization transfer from nearby dipole–dipole-coupled protons. The type of protonated species from which the magnetization originates, however, cannot be distinguished on the basis of this 1D  $^{29}\text{Si}\{^1\text{H}\}$  CP measurement alone. The broad linewidths of the  $^{29}\text{Si}$  MAS resonances ( $\sim 9$  ppm) reflect disordered local  $^{29}\text{Si}$  environments that are common for amorphous silica, due to a large distribution of species, bond lengths, and/or bond angles. Fig. 6(b) shows typical ranges expected for the isotropic  $^{29}\text{Si}$  chemical shifts of siliceous species and organosiloxanes [77,80,81] that may be present in diatoms, especially at the interface of the silica frustule. Previously

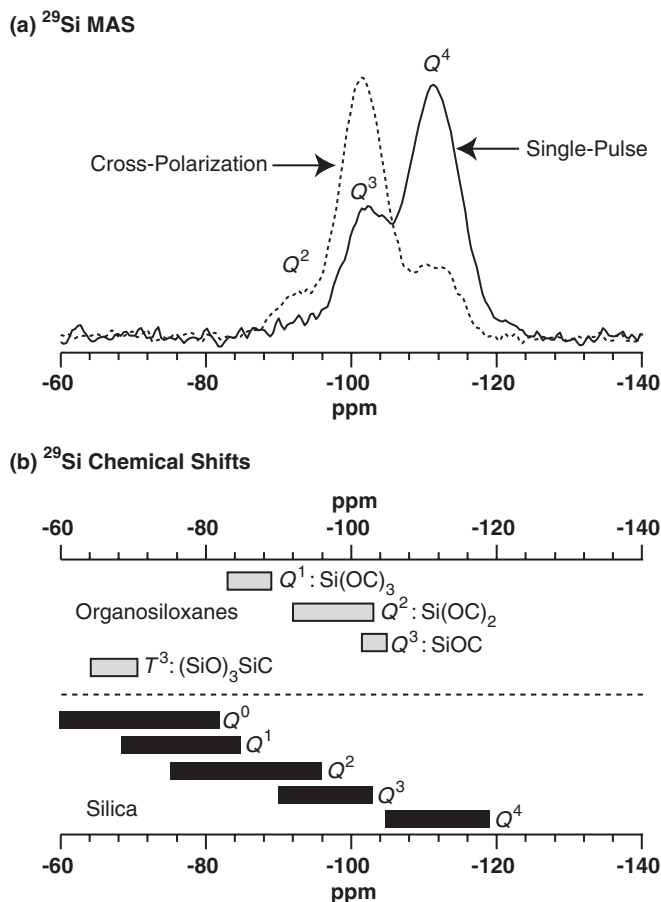


Fig. 6. (a) Solid-state single-pulse (solid line) and cross-polarization (dotted line)  $^{29}\text{Si}$  MAS spectra acquired for a powder sample of  $^{29}\text{Si}$ -enriched, sonicated, and lyophilized diatoms of the species *Thalassiosira pseudonana*. (b)  $^{29}\text{Si}$  NMR chemical shift ranges for various candidate silica and organosiloxane species [77–81].

reported elemental analyses of the frustules of different diatom species have shown that they are composed predominantly of inorganic silica, with some organic species on the exterior frustule surface or occluded within its interior [82,83]. Comparing Figs. 6(a) and (b), it can be seen that it is not possible to infer unambiguously the existence of  $\equiv\text{O}_3\text{Si}-\text{O}-\text{C}-$  type linkages between carbon atoms and  $Q^n$  silica species on the basis of isotropic  $^{29}\text{Si}$  chemical shifts. However, the absence of  $^{29}\text{Si}$  MAS signals over the region  $-65$  to  $-75$  ppm indicates that the existence of so-called ‘trifunctional’ silica species (i.e.,  $T^3$ )  $\equiv\text{O}_3\text{Si}-\text{C}-$ , in which Si atoms are covalently bonded directly to a carbon atom, can be ruled out, within the sensitivity limits of the measurements.

The solid-state  $^{13}\text{C}\{^1\text{H}\}$  CP MAS spectrum in Fig. 7(a) acquired on the same  $^{29}\text{Si}$ ,  $^{13}\text{C}$ -enriched powder sample of diatoms (*T. pseudonana*) as the above shows excellent signal-to-noise, but poor resolution of  $^{13}\text{C}$  signals. Numerous resonances are observed in the spectrum, manifesting the molecular diversity of proteins, sugars, lipids, etc.

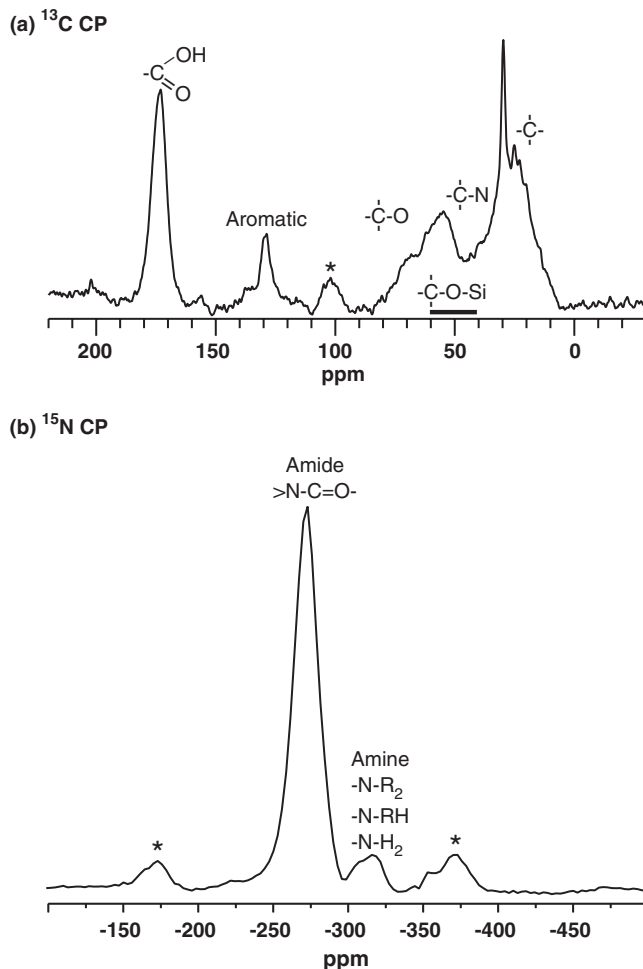


Fig. 7. Solid-state (a)  $^{13}\text{C}$  CP MAS and (b)  $^{15}\text{N}$  CP MAS spectra acquired on a powder sample of  $^{29}\text{Si}$ ,  $^{13}\text{C}$ , and  $^{15}\text{N}$ -enriched diatoms (*T. pseudonana*). The corresponding carbon and nitrogen species are assigned in each spectrum. The asterisks mark spinning sidebands. The  $^{13}\text{C}$  and  $^{29}\text{Si}$  CP MAS spectra of this triply labeled sample are identical to those of the doubly labeled sample measured in Fig. 6(a).

found in this species and organisms in general. This results in overlapping  $^{13}\text{C}$  signals that make it difficult to assign peaks accurately [84], a situation that is even more problematic in the corresponding  $^1\text{H}$  MAS spectrum (see Fig. 8). The poor resolution is unsurprising for the extremely diverse and complicated mixture of organic species present in samples of biological origin. In particular, the existence of hydroxylated amino acid moieties cannot be established from the  $^{13}\text{C}\{^1\text{H}\}$  CP MAS spectrum. Candidate species that have been hypothesized to be present at the frustule surfaces, such as  $\text{RCH}_2-\text{O}-\text{SiO}_3\equiv$  [85], have isotropic  $^{13}\text{C}$  chemical shifts in the vicinity of 55 ppm, which overlaps with  $^{13}\text{C}$  resonances of a variety of other organic species, including  $\text{R}_2\text{CH}-\text{O}-$ ,  $\text{RCH}_2-\text{O}-$  and some terminal  $-\text{CH}_3$  groups. The  $^{15}\text{N}$  CP MAS spectrum in Fig. 7(b) acquired on a triply labeled  $^{29}\text{Si}$ ,  $^{13}\text{C}$ ,  $^{15}\text{N}$ -enriched powder sample of diatoms (*T. pseudonana*) shows excellent signal-to-noise, with two broad resonances at ca.  $-270$  ppm and ca.  $-310$  ppm

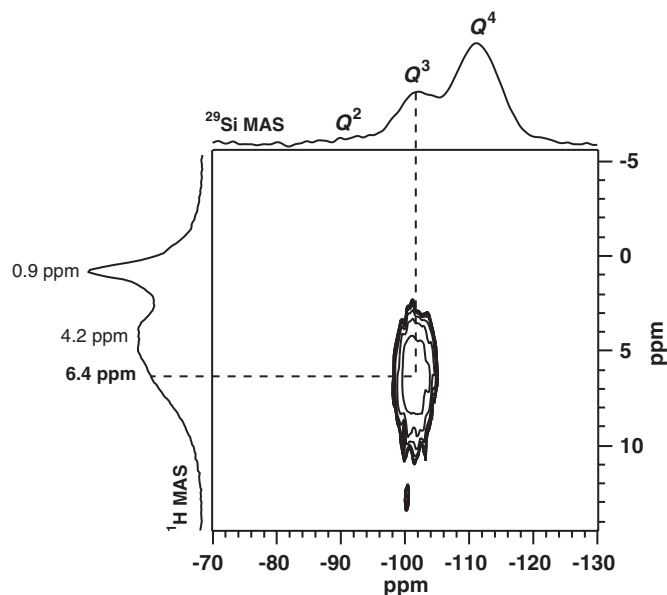


Fig. 8. Solid-state 2D  $^{29}\text{Si}\{^1\text{H}\}$  HETCOR spectrum acquired on the same powder sample of  $^{29}\text{Si},^{13}\text{C}$ -enriched diatoms (*T. pseudonana*), as measured in Figs. 6(a). 1D single-pulse  $^1\text{H}$  and  $^{29}\text{Si}$  MAS spectra are displayed along their corresponding axes to aid the interpretation of the 2D spectrum.

corresponding to amide and amine nitrogen species, respectively [86]. However, as for the  $^{13}\text{C}$  CP MAS spectrum (Fig. 7(a)), the resolution of the 1D  $^{15}\text{N}$  CP MAS spectrum (Fig. 7(b)) is similarly insufficient to identify which amine or amide species are present, especially with respect to their proximities or interactions with the silica frustule. Conventional 1D NMR methods thus provide little information or insight on interfacial structures or moieties at the silica-organic interfaces in diatoms.

More advanced solid-state NMR techniques provide greater selectivity by using heteronuclear dipolar interactions to establish the proximities of different nuclei and their associated chemical moieties. For example, the 2D solid-state  $^{29}\text{Si}\{^1\text{H}\}$  HETCOR spectrum shown in Fig. 8 correlates the isotropic chemical shifts of dipole–dipole-coupled proton and  $^{29}\text{Si}$  species in the same powder sample of the  $^{29}\text{Si},^{13}\text{C}$ -enriched diatom species *T. pseudonana* discussed above. Single-pulse  $^1\text{H}$  and  $^{29}\text{Si}$  MAS spectra are presented along the vertical and horizontal axes, respectively, to aid the interpretation of the 2D HETCOR frequency map. The  $^1\text{H}$  MAS spectrum is composed of signals from a multitude of protonated species, whose resonances severely overlap. (The use of MAS spinning speeds up to 35 kHz failed to improve  $^1\text{H}$  spectral resolution, consistent with the inhomogeneously broadened features.) In broad terms, the  $^1\text{H}$  resonance centered at 0.9 ppm can be attributed to  $-\text{CH}_2-$  or terminal  $-\text{CH}_3$  alkyl groups, whereas the signals in the range of 3–9 ppm represent an assortment of  $^1\text{H}$  species that cannot be resolved. The 1D single-pulse  $^{29}\text{Si}$  MAS spectrum along the horizontal axis is the same as in Fig. 6(a). The 2D  $^{29}\text{Si}\{^1\text{H}\}$

HETCOR spectrum shows a single broad distribution of correlated intensity between the  $Q^3$   $^{29}\text{Si}$  species and what appears to be numerous  $^1\text{H}$  moieties. The very broad intensity correlation in the  $^1\text{H}$  dimension centered at 6.4 ppm may correspond to amide, aromatic, or silanol protons, although a precise determination is not possible due to still insufficient resolution. The absence of correlated signal intensity involving the alkyl  $^1\text{H}$  signals at 0.9 ppm establishes that these species do not experience strong dipole–dipole interactions with  $^{29}\text{Si}$  species in the silica framework. This 2D  $^{29}\text{Si}\{^1\text{H}\}$  HETCOR spectrum measured for the diatoms in Fig. 8 is similar to that acquired from powdered siliceous spicules from a species of sponge [53], which also showed predominant and indefinite interactions between the  $^{29}\text{Si}$  atoms in the biogenic silica framework and most likely hydroxyl protons associated with silanol moieties.

Spectral ambiguities can in principle be overcome by exploiting the higher chemical shift resolution provided by  $^{13}\text{C}$  (~100 ppm range), compared to  $^1\text{H}$  (~10 ppm). Nevertheless, despite the high degrees of isotopic enrichment of both  $^{13}\text{C}$  (85%) and  $^{29}\text{Si}$  (98%) and strong signals in 1D MAS spectra (Figs. 7 and 8) in the powder diatom sample of *T. pseudonana*, no signal intensity was detected in neither a 2D  $^{13}\text{C}\{^{29}\text{Si}\}$  HETCOR experiment nor in an otherwise conventional 1D  $^{13}\text{C}\{^{29}\text{Si}\}$  HHCP MAS measurement. Based on the results discussed in Fig. 4 for analogous  $^{13}\text{C}\{^{15}\text{N}\}$  experiments, the 1D  $^{13}\text{C}\{^{29}\text{Si}\}$  APHH-CP experiment was shown also to provide the highest sensitivity among the heteronuclear of  $X$ – $Y$  polarization transfer methods examined. Applying this pulse sequence (Fig. 4(d)) and after extensive signal-averaging (~146,000 acquisitions, ~80 h), the resulting  $^{13}\text{C}$  APHH-CP spectrum is shown in Fig. 9. The use of  $^{29}\text{Si}$  polarization from silica in a solid diatom frustule as the source of  $^{13}\text{C}$  magnetization serves as a filter to select and detect only those  $^{13}\text{C}$  species at the silica-organic interface and not the vast majority of  $^{13}\text{C}$  species in the enriched diatoms that have no connection with the silica. Clearly the low resultant  $^{13}\text{C}$  signal intensity remains a serious issue associated with the use of heteronuclear dipole–dipole couplings between  $^{13}\text{C}$  and  $^{29}\text{Si}$  moieties to select for species at the silica-organic interface in this sample. This is in spite of efforts to isotopically enrich the organisms, along with the selection of  $X$ – $Y$  polarization transfer methods that maximize the resultant signal intensity.

Nevertheless, although the  $^{13}\text{C}\{^{29}\text{Si}\}$  APHH-CP spectrum in Fig. 9 of the doubly labeled diatoms has relatively poor signal-to-noise (both at 25 °C and at –50 °C), a weak resonance at 171.3 ppm appears to be present (S:N ~2.5). This signal is flanked by two less intense signals at 141 and 203 ppm, which are displaced equally by 4 kHz (the MAS spinning speed) up-field and down-field from the central resonance, which is consistent with their being attributed to spinning sidebands (the relative intensities may be distorted by the poor signal-to-noise). The weak resonance at 171.3 ppm falls in the range of isotropic  $^{13}\text{C}$  chemical

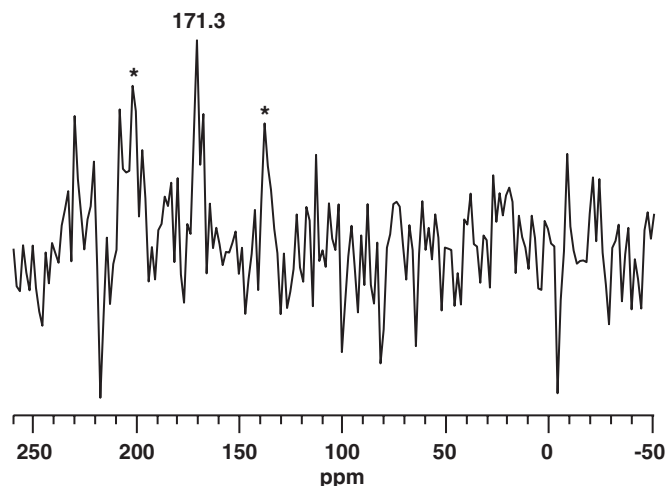


Fig. 9. Solid-state  $^{13}\text{C}$  APHH-CP MAS spectrum acquired at  $-50^\circ\text{C}$  on the same doubly  $^{29}\text{Si}$ ,  $^{13}\text{C}$ -enriched powder sample of diatom species *T. pseudonana* at MAS conditions of 4 kHz with 146,000 acquisitions, as measured in Figs. 6(a) and 8. The asterisks mark presumed spinning sidebands at positions that are separated from the central signal at 171.3 ppm by the sample rotation frequency.

shifts corresponding to carboxylic moieties [84], though this remains to be confirmed. If this is the case, then the presence of carboxylic species near the silica interface may indicate the presence of amino acids, such as glutamate and aspartate. Separate  $^{15}\text{N}\{^{29}\text{Si}\}$  APHH-CP experiments were performed on an otherwise identical powder sample of diatoms additionally enriched in  $^{15}\text{N}$  (98%+), though no  $^{15}\text{N}$  signal was detected after extensive signal averaging ( $\sim 256,000$  acquisitions,  $\sim 140$  h). Based on these results, recent intriguing findings [83] that have identified peptides with post-translationally modified lysine residues (containing numerous nitrogen moieties) to be closely connected with diatom (*C. fusiformis*) silica frustules appear to be beyond the sensitivity limits of these measurements. While differing from the early Hecky model [85], which hypothesized hydroxylated amino acid moieties at biosilica interfaces in diatoms, the presence of carboxylic moieties would nevertheless be consistent with separate studies that have shown the production of relatively high concentrations of glutamate and aspartate in diatoms prior to silicification [87]. The relatively poor signal-to-noise ratio of the  $^{13}\text{C}\{^{29}\text{Si}\}$  APHH-CP necessitates that these findings be confirmed by future measurements with greater signal sensitivity. However, the clear absence of strong interactions between  $^{13}\text{C}$  or  $^{15}\text{N}$  nuclei and  $^{29}\text{Si}$  establishes that the broad correlated distribution of signal intensity in the 2D  $^{29}\text{Si}\{^1\text{H}\}$  HETCOR spectrum (Fig. 8) is predominantly due to interactions with numerous non-organic and presumably silanol proton species.

To our knowledge, these are the first 2D solid-state NMR measurements performed on organic-silica interfaces in diatoms. The possibility exists that relatively non-selective organic-silica interactions exist at the diatom

frustule surface or that, following silica deposition in the living cell, no stable Si–O–C bonds (i.e.,  $\equiv\text{O}_3\text{Si}-\text{O}-\overset{\text{O}}{\underset{\text{O}}{\text{C}}}$ -moieties) are retained (against hydrolysis or otherwise). Under both alkaline and acidic conditions, silicon alkoxides are known to undergo hydrolysis reactions in aqueous solutions [88]. However, solution-state NMR measurements have shown that it is possible to form stable Si–O–C bonds in an aqueous environment using tetraalkylammonium species, which may stabilize Si–O–C moieties [53]. Low frustule surface areas ( $\sim 10\text{ m}^2/\text{g}$ , from  $\text{N}_2$  adsorption measurements), a disordered glass-like silica substrate, complicated distributions of organic components, and exceedingly complex biogenic assembly processes contribute to the challenges inherent in characterizing and understanding biosilica materials and biomineral systems in general.

#### 4. Summary

Heteronuclear dipole–dipole couplings probed by polarization transfer techniques can yield valuable information about the structure of heterogeneous solids, although their feasibilities in complex systems are often limited by low signal sensitivities. Comparisons of the robustness and sensitivity of several different methods for heteronuclear polarization transfer establish that APHH-CP has several advantages over other techniques, including HHCP, VACP, and RACP. Among these methods, the APHH-CP technique, which uses a tangential spin-lock profile, yielded the highest signal intensity for  $^{13}\text{C}\{^1\text{H}\}$  cross-polarization in adamantane. Due to the limited chemical shift range of protons, X–Y polarization transfer between other, often dilute, nuclei can yield improved resolution among dipole–dipole-coupled species, though places even higher demands on the sensitivity of the NMR measurements. A comparison of resultant signal intensities provided by different polarization transfer methods shows that high and comparable sensitivities are obtained from APHH-CP and TEDOR, compared to other approaches, notably the commonly used DCP technique. APHH-CP, in combination with the use of Lee–Goldburg  $^1\text{H}$  decoupling during the contact time, yielded a modestly higher sensitivity than TEDOR. The APHH-CP method may be more suitable for certain applications in complex solids that are otherwise limited by TEDOR's requirement for isolated and 'immobile' dipole–dipole-coupled spin-pairs. Application of 2D  $^{29}\text{Si}\{^1\text{H}\}$  HETCOR, 1D  $^{13}\text{C}\{^{29}\text{Si}\}$  APHH-CP, and 1D  $^{15}\text{N}\{^{29}\text{Si}\}$  APHH-CP methods with Lee–Goldburg  $^1\text{H}$  decoupling to the characterization of a powder sample of isotopically  $^{29}\text{Si}$ ,  $^{13}\text{C}$ , and  $^{15}\text{N}$ -enriched marine diatoms established strong interactions among silanol hydroxyl groups and the silica matrix and weak interactions (if any) involving organic components. Such complicated and interesting heterogeneous solids point to the severe signal sensitivity challenges that still confront efforts to elucidate the properties of complex materials and

important methodological opportunities for the solid-state NMR community.

### Acknowledgments

This paper is dedicated to Prof. Alex Pines on the occasion of his 60th birthday. We thank Dr. Robert Graf and Dr. Almut Rapp for helpful discussions. This work was supported in part by the USARO under grant DAAH04-96-1-0443 and through the Institute for Collaborative Biotechnologies, and the US National Science Foundation Division of Materials Research under award DMR 02-33728. Experiments were conducted using the Central Facilities of the UCSB Materials Research Laboratory supported through MRSEC Program of NSF under award DMR-00-80034.

### References

- [1] S.R. Hartmann, E.L. Hahn, *Phys. Rev.* 128 (1962) 2042–2953.
- [2] A. Pines, M.G. Gibby, J.S. Waugh, *J. Chem. Phys.* 59 (1973) 569–590.
- [3] E.R. Andrew, A. Bradbury, R.G. Eades, *Nature* 182 (1958) 1659.
- [4] J. Schaefer, E.O. Stejskal, *J. Am. Chem. Soc.* 98 (1976) 1031–1032.
- [5] C.S. Blackwell, R.L. Patton, *J. Phys. Chem.* 88 (1984) 6135–6139.
- [6] A.J. Vega, *Solid State Nucl. Magn. Reson.* 1 (1992) 17–32.
- [7] M. Tomaselli, D. deGraw, J.L. Yarger, M.P. Augustine, A. Pines, *Phys. Rev. B* 58 (1998) 8627–8633.
- [8] J.C.C. Chan, M. Bertmer, H. Eckert, *J. Am. Chem. Soc.* 121 (1999) 5238–5248.
- [9] M.A. Eastman, *J. Magn. Reson.* 139 (1999) 98–108.
- [10] S.E. Ashbrook, S.M. Wimperis, *J. Chem. Phys.* 120 (2004) 2719–2731.
- [11] M. Pruski, D.P. Lang, C. Fernandez, J.P. Amoureux, *Solid State Nucl. Magn. Reson.* 7 (1997) 327–331.
- [12] M.G. Munowitz, R.G. Griffin, G. Bodenhausen, T.H. Huang, *J. Am. Chem. Soc.* 103 (1981) 2529–2533.
- [13] P. Caravatti, G. Bodenhausen, R.R. Ernst, *Chem. Phys. Lett.* 89 (1982) 363–367.
- [14] M.G. Zagorski, K. Nakanishi, G.W. Quin, M.S. Lee, *J. Organic Chem.* 53 (1988) 4156–4158.
- [15] X. Wu, K.W. Zilm, *J. Magn. Reson. A* 102 (1993) 205–213.
- [16] R. Sangill, N. Rastrup-Andersen, H. Bildsøe, H.J. Jakobsen, N.C. Nielsen, *J. Magn. Reson. A* 107 (1994) 67–78.
- [17] A. Lesage, S. Steuernagel, L. Emsley, *J. Am. Chem. Soc.* 120 (1998) 7095–7100.
- [18] A. Lesage, L. Duma, D. Sakellariou, L. Emsley, *J. Am. Chem. Soc.* 123 (2001) 5747–5752.
- [19] B. Elena, G. de Paëpe, L. Emsley, *Chem. Phys. Lett.* 398 (2004) 532–538.
- [20] E. Vinogradov, P.K. Madhu, S. Vega, *Top. Curr. Chem.* 246 (2005) 33–90.
- [21] D.E. Demco, S. Kaplan, S. Pausak, J.S. Waugh, *Chem. Phys. Lett.* 30 (1975) 77–82.
- [22] J. Schaefer, R.A. McKay, E.O. Stejskal, *J. Magn. Reson.* 34 (1979) 443–447.
- [23] E.O. Stejskal, J. Schaefer, R.A. McKay, *J. Magn. Reson.* 57 (1984) 471–485.
- [24] J. Schaefer, E.O. Stejskal, J.R. Garbow, R.A. McKay, *J. Magn. Reson.* 59 (1984) 150–156.
- [25] H. Kim, T.A. Cross, R. Fu, *J. Magn. Reson.* 168 (2004) 147–152.
- [26] A.W. Hing, S. Vega, J. Schaefer, *J. Magn. Reson. A* 103 (1993) 151–162.
- [27] C.A. Fyfe, K.T. Mueller, H. Grondey, K.C. Wong-Moon, *J. Phys. Chem.* 97 (1993) 13484–13495.
- [28] B.-J. van Rossum, C.P. de Groot, V. Ladizhansky, S. Vega, H.J.M. de Groot, *J. Am. Chem. Soc.* 122 (2000) 3465–3472.
- [29] M. Edén, A. Brinkmann, H. Luthman, L. Eriksson, M.H. Levitt, *J. Magn. Reson.* 144 (2000) 266–279.
- [30] J.D. Mao, K. Schmidt-Rohr, *J. Magn. Reson.* 162 (2003) 217–227.
- [31] X. Zhao, W. Hoffbauer, J. Schmedt auf der Günne, M.H. Levitt, *Solid State Nucl. Magn. Reson.* 26 (2004) 57–64.
- [32] S.V. Dvinskikh, H. Zimmermann, A. Maliniak, D. Sandström, *J. Chem. Phys.* 122 (2005) 044512.
- [33] S.V. Dvinskikh, V. Castro, D. Sandström, *Phys. Chem. Chem. Phys.* 7 (2005) 607–613.
- [34] K. Schmidt-Rohr, H.W. Spiess, *Multidimensional Solid-State NMR and Polymers*, Academic Press, London, 1994.
- [35] C.P. Grey, A.P.A.M. Eijkelenboom, W.S. Veeman, *Solid State Nucl. Magn. Reson.* 4 (1995) 113–120.
- [36] C.P. Grey, A.J. Vega, *J. Am. Chem. Soc.* 117 (1995) 8232–8242.
- [37] T. Gullion, J. Schaefer, *J. Magn. Reson.* 81 (1989) 196–200.
- [38] J.L. White, L.W. Beck, J.F. Haw, *J. Am. Chem. Soc.* 114 (1992) 6182–6189.
- [39] H.-M. Kao, H. Liu, J.-C. Jiang, S.-H. Lin, C.P. Grey, *J. Phys. Chem. B* 104 (2000) 4923–4933.
- [40] C.A. Fyfe, H. Grondey, A.C. Diaz, G.T. Kokotailo, Y. Feng, Y. Huang, K.C. Wong-Moon, K.T. Mueller, H. Strobl, A.R. Lewis, *Stud. Surf. Sci. Catal.* 97 (1995) 1–10.
- [41] C.A. Fyfe, A.C. Diaz, H. Grondey, A.R. Lewis, H. Förster, *J. Am. Chem. Soc.* 127 (2005) 7543–7558.
- [42] C.A. Click, R.A. Assink, C.J. Brinker, S.J. Naik, *J. Phys. Chem. B* 104 (2000) 233–236.
- [43] A.J. Vega, *J. Am. Chem. Soc.* 110 (1988) 1049–1054.
- [44] M.T. Janicke, C.C. Landry, S.C. Christiansen, D. Kumar, G.D. Stucky, B.F. Chmelka, *J. Am. Chem. Soc.* 110 (1998) 6940–6951.
- [45] M.T. Janicke, C.C. Landry, S.C. Christiansen, S. Birtalan, G.D. Stucky, B.F. Chmelka, *Chem. Mater.* 11 (1999) 1342–1351.
- [46] S.C. Christiansen, D. Zhao, M.T. Janicke, C.C. Landry, G.D. Stucky, B.F. Chmelka, *J. Am. Chem. Soc.* 123 (2001) 4519–4529.
- [47] J. Trébosc, J.W. Wiench, S. Huh, V.S.-Y. Lin, M. Pruski, *J. Am. Chem. Soc.* 127 (2005) 3057–3068.
- [48] D.H. Brouwer, P.E. Kristiansen, C.A. Fyfe, M.H. Levitt, *J. Am. Chem. Soc.* 127 (2005) 542–543.
- [49] N. Hedin, R. Graf, S.C. Christiansen, C. Gervais, R.C. Hayward, J. Eckert, B.F. Chmelka, *J. Am. Chem. Soc.* 126 (2004) 9425–9432.
- [50] C.A. Fyfe, H. Gies, Y. Feng, *J. Am. Chem. Soc.* 111 (1989) 7702–7707.
- [51] C.A. Fyfe, H. Gies, Y. Feng, H. Grondey, G.T. Kokotailo, *J. Am. Chem. Soc.* 112 (1990) 3264–3270.
- [52] R.E. Morris, S.J. Weigel, N.J. Henson, L.M. Bull, M.T. Janicke, B.F. Chmelka, A.K. Cheatham, *J. Am. Chem. Soc.* 116 (1994) 11849–11855.
- [53] S.D. Kinrade, K.J. Maa, A.S. Schach, T.A. Sloan, C.T.G. Knight, *J. Chem. Soc. Dalton Trans.* 18 (1999) 3149–3150.
- [54] J.C. Weaver, L.I. Pietrasanta, N. Hedin, B.F. Chmelka, P.K. Hansma, D.E. Morse, *J. Struct. Biol.* 144 (2003) 271–281.
- [55] C. Jaeger, N.S. Groom, E.A. Bowe, A. Horner, M.E. Davies, R.C. Murray, M.J. Duer, *Chem. Mater.* 17 (2005) 3059–3061.
- [56] E.D. Segal, J. Cha, J. Lo, S. Falkow, L.S. Tompkins, *Proc. Natl. Acad. Sci.* 96 (1999) 14559–14564.
- [57] N. Kröger, R. Deutzmann, M. Sumper, *Science* 286 (1999) 1129–1132.
- [58] R.R.L. Guillard, J. Ryther, *Can. J. Microbiol.* 8 (1962) 229–239.
- [59] R.R.L. Guillard, in: W.L. Smith, M.H. Chanley (Eds.), *Culture of Marine Invertebrate Animals*, Plenum Press, New York, 1975, pp. 26–60.
- [60] D.M. Nelson, M.A. Brzezinski, *Mar. Ecol. Prog. Ser.* 62 (1990) 283–292.

- [61] E.O. Stejskal, J. Schaefer, J.S. Waugh, *J. Magn. Reson.* 28 (1977) 105–112.
- [62] D. Marks, S. Vega, *J. Magn. Reson. A* 118 (1996) 157–172.
- [63] A. Verhoeven, R. Verel, B.H. Meier, *Chem. Phys. Lett.* 266 (1997) 465–472.
- [64] S. Hediger, B.H. Meier, R.R. Ernst, *Chem. Phys. Lett.* 213 (1993) 627–635.
- [65] O.B. Peersen, X. Wu, I. Kustanovich, S.O. Smith, *J. Magn. Reson. A* 104 (1993) 334–339.
- [66] O.B. Peersen, X. Wu, S.O. Smith, *J. Magn. Reson. A* 106 (1994) 127–131.
- [67] G. Metz, X. Wu, S.O. Smith, *J. Magn. Reson. A* 110 (1994) 219–227.
- [68] S. Hediger, B.H. Meier, N.D. Kurur, G. Bodenhausen, R.R. Ernst, *Chem. Phys. Lett.* 223 (1994) 283–288.
- [69] S. Hediger, B.H. Meier, R.R. Ernst, *Chem. Phys. Lett.* 240 (1995) 449–456.
- [70] P. Hodgkinson, A. Pines, *J. Chem. Phys.* 107 (1997) 8742–8751.
- [71] N.C. Nielsen, H. Bildsøe, H.J. Jakobsen, M.H. Levitt, *J. Chem. Phys.* 101 (1994) 1805–1812.
- [72] X. Wu, K.W. Zilm, *J. Magn. Reson. A* 104 (1993) 154–165.
- [73] B.Q. Sun, P.R. Costa, R.G. Griffin, *J. Magn. Reson. A* 112 (1995) 191–198.
- [74] M. Bjerring, N.C. Nielsen, *Chem. Phys. Lett.* 382 (2003) 671–678.
- [75] M. Baldus, D.G. Geurts, S. Hediger, B.H. Meier, *J. Magn. Reson. A* 118 (1996) 140–144.
- [76] M. Lee, W.I. Goldberg, *Phys. Rev.* 140 (1965) A1261–A1271.
- [77] G. Engelhardt, D. Michel, *High Resolution Solid State NMR of Silicates and Zeolites*, Wiley, New York, 1987.
- [78] R. Bertermann, N. Kröger, R. Tacke, *Anal. Bioanal. Chem.* 375 (2003) 630–634.
- [79] K. Lutz, C. Gröger, M. Sumper, E. Brunner, *Phys. Chem. Chem. Phys.* 7 (2005) 2812–2815.
- [80] L.W. Kelts, N.J. Armstrong, *J. Mater. Res.* 4 (1989) 423–433.
- [81] E.A. Williams, in: S. Patai, Z. Rappoport (Eds.), *The Chemistry of Organic Silicon Compounds*, Wiley, New York, 1998, pp. 511–554.
- [82] D.M. Swift, A.P. Wheeler, *J. Phycol.* 28 (1992) 202–209.
- [83] N. Kröger, R. Deutzmann, M. Sumper, *J. Biol. Chem.* 276 (2001) 26066–26070.
- [84] E. Pretsch, T. Clerc, J. Seibl, W. Simon, *Tables of Spectral Data for Structure Determination of Organic Compounds*, Springer, Berlin, 1983.
- [85] R.E. Hecky, K. Mopper, P. Kilham, E.T. Degens, *Marine Biol.* 19 (1973) 323–331.
- [86] M. Witkowski, L. Stefaniak, G.A. Webb, *Nitrogen NMR*, Academic Press, London, 1993.
- [87] J. Coombs, B.E. Volcani, *Planta* 82 (1968) 280–292.
- [88] C.J. Brinker, G.W. Scherer, *Sol–Gel Science: The Physics and Chemistry of Sol–Gel-Processing*, Academic Press, New York, 1990.